A study on hydrodynamics of the air cushion of a high-speed PACSCAT

Zhiqun Guo[a], Hongde Qin[a,*], Q.W. Ma[a,b,*]

[a] College of Shipbuilding Engineering, Harbin Engineering University, Harbin, China

[b] School of Engineering and Mathematical Sciences, City University London, London, UK

Abstract

This paper presents an approximate but efficient method for modeling the hydrodynamics and seakeeping performance of partial air cushion supported catamaran (PACSCAT) with planing demihulls. This method takes into account of the effects of the waves on the air-water interface under the air cushion induced by the pulsating pressure in the cushion and by the demihulls, which are ignored by existing approximate methods. Specifically, the new developments are made in two aspects. One is that the governing equations of the heave and pitch motions of the PACSCAT are derived to include the effects of the waves under the air cushion due to the pulsating pressure and the demihulls. Another one is that an approximate method is developed for evaluating the waves due to the pulsating pressure. Better agreement between the experimental data and the numerical results for pressure is achieved.

Keywords: Partial air cushion supported catamaran (PACSCAT); air cushion; hydrodynamics; seakeeping; 2.5D theory

* Corresponding authors
Hongde Qin e-mail address: qinhongde@hrbeu.edu.cn; QW Ma e-mail address: q.ma@city.ac.uk

Nomenclature

A	Waterplane area of the air cushion
B	Beam of an air cushion used for computation
B_{c}	Beam of PACSCAT
b	Beam of the air cushion under PACSCAT
C_{n}	Air flow contraction coefficient
F_i^{R}	Sum of radiation and hydrostatic restoring forces / moments of demihulls, $i = 3{,}5$
F_i^{W}	Sum of incident and diffraction wave force / moment, $i = 3{,}5$
F_{rL}	Length (of water line) Froude number
g	Gravitational acceleration
h	Height of the air cushion (from the interface to cushion chamber ceiling)
h_i	Height from free surface to underneath of stern / bow seals at equilibrium, $i = 1{,}2$
I_{55}	Moment of inertia for pitch
k	Wave number
L_{O}	Overall length of PACSCAT
L	Length of water line
l	Length of the air cushion
M	Mass of PACSCAT
N_{in}	Number of inlet holes in the air cushion chamber
p	Overpressure in the air cushion
$\tilde{p}$	Pulsating pressure in the air cushion
p_0	Overpressure in the air cushion at equilibrium
p_{a}	Atmospheric pressure
$\tilde{p}_j$	Discretization of pulsating pressure $\tilde{p}$
$\tilde{p}_{\mathrm{r}}$	Rectangular pulsating pressure patch with unit amplitude
Q_0	Inflow / Outflow rate (discharge) at equilibrium
Q_{in}	Overall inflow rate
q_i^{in}	Inflow rate at ith inlet hole, $i = 1{,}2, \ldots, N_{\mathrm{in}}$
Q_{out}	Overall outflow (air leakage) rate
q_i^{out}	Outflow rate at ith outlet vent, $i = 1{,}2$ denote outflow from gap under stern and bow seal, respectively
t	Time
T_{c}	demihull draught at COG (in the side of the air cushion)
T_{o}	demihull draught at COG (in the outside)
U	Speed of the PACSCAT
x_{g}	x-coordinate of COG
x_i	x-coordinate of ith inlet hole / outlet vent at vehicle-accompanied coordinate system
y_{g}	y-coordinate of COG
z_{g}	Vertical COG (from baseline)
α	Pressure coefficient with respect to the time-variant term
β	Pressure coefficient with respect to the spatial variant term
γ	Ratio of specific heats for air, the value is 1.4
Δ_{s}	Displacement of demihulls (cushion-on, zero speed)
ξ	x-coordinate of the pressure patch $\tilde{p}$
ζ	Wave elevation on free surface in the air cushion
$\bar{\zeta}$	Sectional-averaged value of ζ
$\bar{\bar{\zeta}}$	Spatial-averaged value of ζ
$\hat{\bar{\zeta}}$	Spatial-weighted-averaged value of ζ
ζ_{H}	Waves excited by demihulls
ζ_{h}	Amplitude of waves ζ_{H}
$\zeta_{\mathrm{h}j}$	Amplitudes of induced waves by heave ($j = 3$), pitch ($j = 5$) or incident wave ($j = 7$) of demihulls
ζ_{I}	Incident waves
ζ_{a}	Amplitude of incident waves ζ_{I} in the air cushion
ζ_j	Free surface elevation due to the pressure patch $\tilde{p}_j$
ζ_{P}	Waves excited by pulsating pressure $\tilde{p}$
ζ_{p}	Amplitude of waves ζ_{P}
$\zeta_{\mathrm{p}j}$	Amplitudes of induced waves by spatial-invariant pulsating pressure ($j = 1$), or spatial-variant pulsating pressure ($j = 2$)
ζ_{r}	Free surface elevation due to pressure patch $\tilde{p}_{\mathrm{r}}$
η_i	Heave, pitch of PACSCAT, $i = 3, 5$, respectively
η_i^{s}	Amplitude of motions $\eta_i, i = 3, 5$ for heave and pitch
θ	Trim of PACSCAT
λ	Wave length
τ	Reduced frequency
ρ_0	Density of air at equilibrium pressure $p_0 + p_{\mathrm{a}}$
ρ_{a}	Density of atmosphere at pressure p_{a}
ρ_{w}	Density of water
ω	Encountered wave frequency
ω_0	Natural wave frequency
φ	Water velocity potential for air-water interaction
ψ_j	Water velocity potential due to unit heave ($j = 3$), pitch ($j = 5$) of demihulls, diffraction wave ($j = 7$)

1. Introduction

Some new types of surface effect ships (SES), such as Harley SES [1] and partial air cushion supported catamarans (PACSCAT) [2], have been proposed recently. Compared with conventional planing catamarans that have an open channel between demihulls, the PACSCAT is partially supported by pressurized air contained in the plenum channel surrounded with planing demihulls and end seals (Fig. 1). Model tests and sea trials suggest that the PACSCAT has superiority of lower resistance and better seakeeping performance as compared to planing catamarans, while the maneuverability outperforms hovercrafts [3].

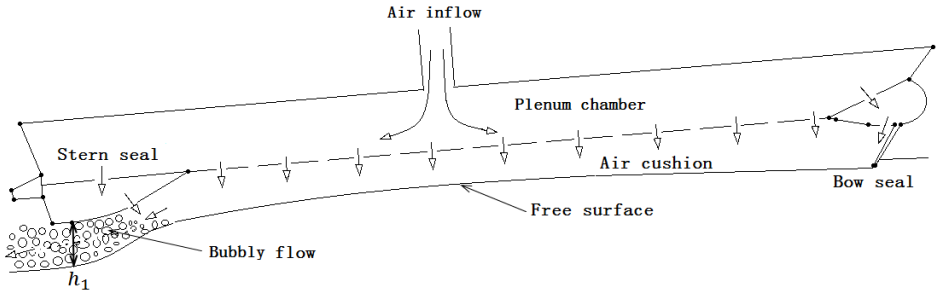

Fig. 1. Longitudinal profile of the PACSCAT model and air flow sketch.

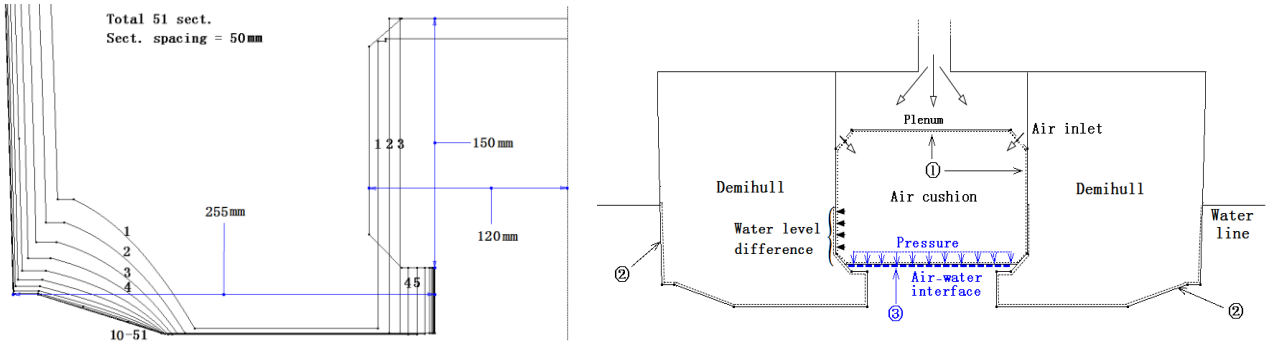

(a) Body plan (b) Skech of a transverse section

Fig. 2. Body plan and illustration of the air cushion, demihulls and the interface under air cushion of PACSCAT.

In general, the seakeeping motion of the PACSCAT, like other SES, is affected by hydrodynamics of demihulls (if applicable), air dynamics and hydrodynamics of the air cushion (Fig. 2). The hydrodynamics of the air cushion refers to the waves generated by the pulsating air pressure. The three effects of the hydrodynamics, air dynamics and hydrodynamics of the air cushion are coupled with each other. Apart from these, the hydrodynamics of demihulls and air dynamics of the air cushion directly influence the motions of the craft.

Currently, the numerical methods for analyzing seakeeping performance of the SES or PACSCAT could be grouped into two categories: computational methods and approximate methods. The computational methods, such as Rankine source method [4,5] and RANS method [6,7], may be

able to take into account all dynamic effects, but they require considerable amount of computational resources and can take long computational time [3,8].

The approximate methods have an advantage of high computational efficiency, but many of them more or less have shortcomings due to approximations and assumptions they are based on. For example, most approximate methods did not take into account of the hydrodynamics of demihulls [9,10] or just directly added hydrodynamic coefficients to air dynamic ones [11,12] without fully accounting for the aero-hydrodynamic coupled effects. Many researchers [9-13] adopted the Froude-Krylov hypothesis, that is, the effect of the incident wave on the pressure of the air cushion is only considered but ignoring the effect of pulsating air pressure and demihulls on waves. However, it has been reported by Doctors [14,15] and Kim and Tsakonas [16] that the waves due to the pressure in the air cushion can significantly affect the behavior of SESs.

Moreover, many approximate methods for dealing with the hydrodynamics of the air cushion are based on the assumption that the air cushion is a rectangular pulsating pressure patch without consideration of demihulls [14-17]. Obviously in such models the radiation waves induced by the pulsating air pressure are allowed to freely propagate in all directions to the far field, which may be inconsistent with the fact that demihulls prevent or disturb the outgoing waves. Ogilvie [18] studied the 2D wavemaker-with-lip (2D air cushion with sidewalls) problem, and came to a conclusion that it may be cautious about ignoring the sidewall effect in general, which indicates that the sidewall effect on waves caused by the pulsating air pressure might be important and requires to be considered. Evidently, if one wishes to precisely evaluate the waves with the sidewall effect due to a pulsating pressure patch, a mixed boundary value problem (BVP) should be solved, which requires lots of computational resources.

Very recently, Guo et al. [3] proposed an efficient seakeeping analysis method for the PACSCAT, which is formed by combining the 2.5D methods for solving hydrodynamics of demihulls with simplified wave-equation for air dynamics of the air cushion. But Guo et al. [3] did not take the hydrodynamics of the pulsating air pressure and demihulls on waves into account. To overcome this shortcoming, Guo et al. [8] proposed a novel 2.5D method that can solve the mixed BVP for evaluating the waves due to the pulsating air pressure. However, as indicated by Guo et al. [19], the 2.5D method is valid only when the advancing speed and the length to beam ratio of the air cushion to be sufficient high, which restricts its application range. In contrast, the 3D linear potential method [14,16] does not make any limitations on accounting for the waves induced by the pulsating air pressure, i.e. the advancing speed can be slow and the cushion beam is allowed to be much larger than the cushion length.

In this paper, the authors intend to provide an efficient 3D linear approach for approximately

estimating the waves due to the pulsating air pressure in the cushion with consideration of the sidewall effect, to improve the seakeeping analysis model presented in Guo et al. [3]. In this improved model, the demihulls are simplified as thin sidewalls when forming the equations accounting for the sidewall effect of the waves induced by the pulsating air pressure. When evaluating the hydrodynamic characteristics of demihulls, the real geometry of demihulls is used without the simplification.

2. Mathematical formulation for the motions of PACSCAT and the pressure in the air cushion

2.1 Principal parameters for the PACSCAT model

The geometrical details and model tests on the PACSCAT have been presented by Guo et al. [3]. Main characteristics and the body plan of the model-scale PACSCAT are given Figs. 1-2 and in Table 1. More details can be found in the cited paper. Some equations were also presented in the cited paper but will be given in this section for completeness.

Table 1

Model principal parameters [3]

M	145 kg	I_{55}	77.4 kg·m^2		$F_{rL}=0.73$	$F_{rL}=1.0$
L_O	3.0 m	L	2.5 m	p_0	760 Pa	510 Pa
l	2.5 m	B_c	0.7 m	T_c	2.4 cm	4.4 cm
b	0.24 m	x_g	-0.08 m from midship	T_o	10.0 cm	9.5 cm
y_g	0.0 m	z_g	0.096 m from baseline	θ	3.42 deg	3.47 deg
Q_0	150 m^3/h	$(\partial Q_{in}/\partial p)_0$	-7.2E-4 m^3/(s · Pa)	ζ_a	2.5 cm	2.5 cm

In order to analyze the seakeeping properties of the PACSCAT, one needs to evaluate the pressure in the air cushion and hydrodynamic forces on demihulls. For this purpose, one needs to consider three BVPs, i.e., the air dynamic BVP (marked as ① in Fig. 2) for solving pressure in the air cushion, the hydrodynamic BVP about water waves on the air-water interface (marked as ③ in Fig. 2) caused by the pulsating pressure in the air cushion, and the BVP about hydrodynamics of demihulls (marked as ② in Fig. 2). The first BVP will be discussed in the next subsection while the second and third will be discussed in Section 3.

2.2 Air dynamic BVP for the air cushion

The cushion air dynamic BVP has been decribed and approximately solved in Guo et al. [3], where the hydrodynamics of the air cushion was not considered and only incoming wave elevation was accounted for. The similar method for solving the BVP will be followed but the particular attention

will be paid to the difference from the previous work.

As shown in Guo et al. [3], the pulsating pressure in the air cushion can be written as

$$\tilde{p}(x,t) = p - p_0 = \mathrm{Re}\{p_0\alpha \mathrm{e}^{\mathrm{i}\omega t} - \rho_0\beta \mathrm{e}^{\mathrm{i}\omega t}\sin(\pi x/l)\} \quad (1)$$

where Re means to take the real part of the function and will be dropped for simplicity. Hereafter, all other variables will be dealt with in the same way.

As explained by Guo et al. [3] about their Eq. (16), one can obtain the similar equation below from the equations satisfied by the pressure

$$\frac{\mathrm{i}\omega h}{\gamma(p_0+p_\mathrm{a})}p_0 A\alpha \mathrm{e}^{\mathrm{i}\omega t} + A\dot{\eta}_3 + (Q_\mathrm{out} - Q_\mathrm{in}) - \left(2\mathrm{i}\omega b\zeta_\mathrm{a}\sin\left(\frac{kl}{2}\right)/k + \mathrm{i}\omega A\left(\bar{\bar{\zeta}}_\mathrm{p} + \bar{\bar{\zeta}}_\mathrm{h}\right)\right)\mathrm{e}^{\mathrm{i}\omega t} = 0 \quad (2)$$

The difference between Eq. (2) here and Eq. (16) in Guo et al. [3] lies in the last term associated with the air-water interface elevation under the air cushion. The elevation due only to the incident wave in Eq. (16) of Guo et al. [3] is replaced by the total elevation in Eq. (2) here. The total elevation ($\zeta(x,y,t)$) consists of the incident wave (ζ_I), the wave due to the pulsating pressure in the air cushion (ζ_P), and the diffraction and radiation waves of the hulls (ζ_H), that is (see Appendix I for more details)

$$\zeta(x,y,t) = \zeta_\mathrm{I} + \zeta_\mathrm{P} + \zeta_\mathrm{H} = (\zeta_\mathrm{a}\mathrm{e}^{\mathrm{i}kx} + \zeta_\mathrm{p}(x,y) + \zeta_\mathrm{h}(x,y))\,\mathrm{e}^{\mathrm{i}\omega t} \quad (3)$$

where ζ_a, k are the amplitude and wave number of ζ_I, respectively; $\zeta_\mathrm{p}(x,y)$ is the complex amplitude of ζ_P; $\zeta_\mathrm{h}(x,y)$ is the complex amplitude of ζ_H. $\bar{\bar{\zeta}}_\mathrm{p}$ and $\bar{\bar{\zeta}}_\mathrm{h}$ in Eq. (2) are defined by

$$\begin{cases} \bar{\bar{\zeta}}_\mathrm{p} = \frac{1}{A}\int_{-\frac{l}{2}}^{\frac{l}{2}}\int_{-\frac{b}{2}}^{\frac{b}{2}}\zeta_\mathrm{p}(x,y)\mathrm{d}y\,\mathrm{d}x \\ \bar{\bar{\zeta}}_\mathrm{h} = \frac{1}{A}\int_{-\frac{l}{2}}^{\frac{l}{2}}\int_{-\frac{b}{2}}^{\frac{b}{2}}\zeta_\mathrm{h}(x,y)\mathrm{d}y\,\mathrm{d}x \end{cases} \quad (4)$$

According to the expression of air leakage given in Guo et al. [3], and taking the interface waves (Eq.(3)) into account, the overall air leakage can be linearized as follows

$$Q_\mathrm{out} \cong Q_0\left(1 + \frac{\alpha \mathrm{e}^{\mathrm{i}\omega t}}{2} - \frac{\rho_0\beta \mathrm{e}^{\mathrm{i}\omega t}\sin\left(-\frac{l}{2}\frac{\pi}{l}\right)}{2p_0}\right) + \frac{\eta_3 + \frac{l}{2}\eta_5}{h_1}Q_0 - \frac{\left(\zeta_\mathrm{a}\mathrm{e}^{-\mathrm{i}k\frac{l}{2}} + \bar{\zeta}_\mathrm{p}\left(-\frac{l}{2}\right) + \bar{\zeta}_\mathrm{h}\left(-\frac{l}{2}\right)\right)\mathrm{e}^{\mathrm{i}\omega t}}{h_1}Q_0 \quad (5)$$

where $Q_0 = C_\mathrm{n}h_1 b\sqrt{2p_0/\rho_0}$ is the air leakage via clearance under stern lobes at equilibrium; $\bar{\zeta}_\mathrm{p}(x) = \frac{1}{b}\int_{-b/2}^{b/2}\zeta_\mathrm{p}(x,y)\mathrm{d}y$, $\bar{\zeta}_\mathrm{h}(x) = \frac{1}{b}\int_{-b/2}^{b/2}\zeta_\mathrm{h}(x,y)\mathrm{d}y$ are sectional-averaged amplitude of the interface elevation due to the pulsating air pressure and demihulls, respectively. This equation is similar to Eq.(26) in Guo et al. [3] but with additional contribution of the interface elevation induced by the wave due to the pulsating pressure in the air cushion and the diffraction and radiation waves of the hulls. Then the air outflow and inflow difference can be written as

$$Q_\mathrm{out} - Q_\mathrm{in} = \left(\frac{Q_0}{2} - p_0\left(\frac{\partial Q_\mathrm{in}}{\partial p}\right)_0\right)\alpha \mathrm{e}^{\mathrm{i}\omega t} + \frac{Q_0\rho_0\beta \mathrm{e}^{\mathrm{i}\omega t}}{2p_0} + \frac{\eta_3 + \frac{\eta_5 l}{2}}{h_1}Q_0 - \frac{\left(\zeta_\mathrm{a}\mathrm{e}^{-\mathrm{i}\frac{kl}{2}} + \bar{\zeta}_\mathrm{p}\left(-\frac{l}{2}\right) + \bar{\zeta}_\mathrm{h}\left(-\frac{l}{2}\right)\right)\mathrm{e}^{\mathrm{i}\omega t}}{h_1}Q_0 \quad (6)$$

Inserting Eq. (6) into Eq. (2) leads to

$$\begin{aligned}&\left(\frac{\mathrm{i}\omega hA}{\gamma(p_0+p_\mathrm{a})}+\frac{Q_0}{2p_0}-\left(\frac{\partial Q_\mathrm{in}}{\partial p}\right)_0\right)p_0\alpha\mathrm{e}^{\mathrm{i}\omega t}+\frac{Q_0}{2p_0}\rho_0\beta\mathrm{e}^{\mathrm{i}\omega t}=-\frac{\eta_3+\eta_5 l/2}{h_1}Q_0\\&-A\dot{\eta}_3+\left(\frac{2\mathrm{i}\omega b\zeta_\mathrm{a}\sin\frac{kl}{2}}{k}+\mathrm{i}\omega A\left(\bar{\bar{\zeta}}_\mathrm{p}+\bar{\bar{\zeta}}_\mathrm{h}\right)+\frac{\zeta_\mathrm{a}\mathrm{e}^{-\mathrm{i}\frac{kl}{2}}+\bar{\zeta}_\mathrm{p}\left(-\frac{l}{2}\right)+\bar{\zeta}_\mathrm{h}\left(-\frac{l}{2}\right)}{h_1}Q_0\right)\mathrm{e}^{\mathrm{i}\omega t}\end{aligned}\tag{7}$$

This equation corresponds to Eq. (29a) in Guo et al. [3] but with the incident wave elevation replaced by the total wave elevation.

Following the similar argument, one can obtain the equation below corresponding to Eq. (29b) in Guo et al. [3]

$$\begin{aligned}&\frac{Q_0}{2p_0}p_0\alpha\mathrm{e}^{\mathrm{i}\omega t}+\left(\frac{Ah}{2\mathrm{i}\omega}\left(\frac{\pi^2}{\rho_0 l^2}-\frac{\omega^2}{\gamma(p_0+p_\mathrm{a})}\right)+\frac{\left(Q_0-p_0\left(\frac{\partial Q_\mathrm{in}}{\partial p}\right)_0\right)}{2p_0}\right)\rho_0\beta\mathrm{e}^{\mathrm{i}\omega t}=-\frac{\eta_3+\eta_5 l/2}{h_1}Q_0\\&-\frac{2Al}{\pi^2}\dot{\eta}_5+\left(\frac{2\zeta_\mathrm{a}kAl\omega\cos\frac{kl}{2}}{\pi^2-k^2l^2}-\mathrm{i}\omega A\left(\hat{\bar{\zeta}}_\mathrm{p}+\hat{\bar{\zeta}}_\mathrm{h}\right)+\frac{\zeta_\mathrm{a}\mathrm{e}^{-\mathrm{i}\frac{kl}{2}}+\bar{\zeta}_\mathrm{p}\left(-\frac{l}{2}\right)+\bar{\zeta}_\mathrm{h}\left(-\frac{l}{2}\right)}{h_1}Q_0\right)\mathrm{e}^{\mathrm{i}\omega t}\end{aligned}\tag{8}$$

where

$$\begin{cases}\hat{\bar{\zeta}}_\mathrm{p}=\frac{1}{A}\int_{-\frac{l}{2}}^{\frac{l}{2}}\int_{-\frac{b}{2}}^{\frac{b}{2}}\zeta_\mathrm{p}(x,y)\sin(\pi x/l)\,\mathrm{d}y\,\mathrm{d}x\\\hat{\bar{\zeta}}_\mathrm{h}=\frac{1}{A}\int_{-\frac{l}{2}}^{\frac{l}{2}}\int_{-\frac{b}{2}}^{\frac{b}{2}}\zeta_\mathrm{h}(x,y)\sin(\pi x/l)\,\mathrm{d}y\,\mathrm{d}x\end{cases}\tag{9}$$

3. Waves on the air-water interface and hydrodynamic forces on the demihulls

The evaluation of the terms associated with the waves under the air cushion induced by the pulsating air pressure and demihulls, as well as the hydrodynamics of demihulls, will be discussed in this section. The methods are based on linearized assumption, which are formulated into two BVPs as given in Appendix I: hydrodynamic BVP for the pulsating air pressure and hydrodynamic BVP for demihulls, respectively. In addition, we aim for an efficient approach and so necessary simplification will be made like other papers in literature.

3.1 Hydrodynamic BVP for the pulsating air pressure

The pulsating pressure in the air cushion is modeled as a rectangular pressure patch $\tilde{p}(x,t)$ (Eq. (1)) confined by two demihulls oscillating and traveling with a constant speed U as discussed in Appendix I and illustrated in Fig. 3. In Appendix I, it is also justified that the demihulls are replaced by two thin plates (so hereafter called as "sidewall"). It is worth noting that the static air pressure p_0 will make the average interface lower than the free surface. For the sake of simplicity, following Guo et al. [3], the water level difference in this paper is ignored and the interface is approximately set on the same level as the free surface. This is rational due to that the wall-sided demihulls as well as the water level of the interface has little influence on the dynamics of the pulsating air pressure.

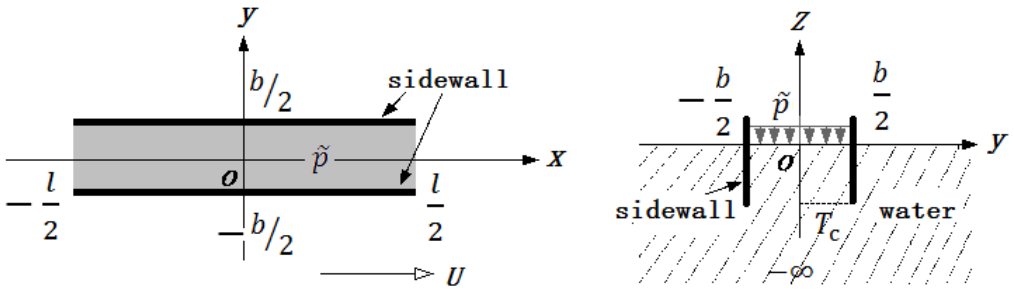

Fig. 3. Sketch of pulsating pressure with sidewalls (Left: top view; Right: front view).

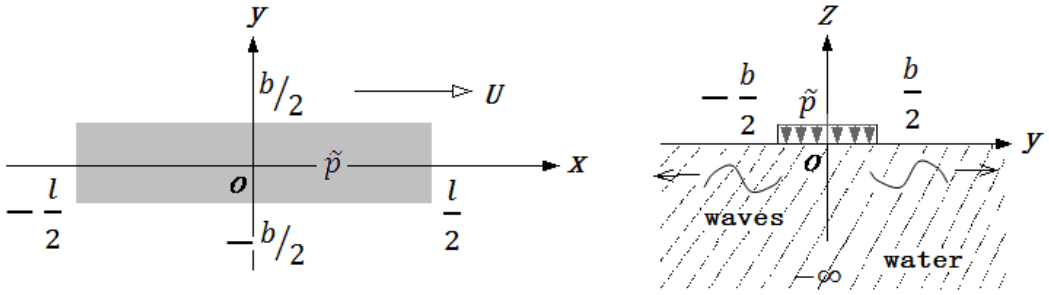

Fig. 4. Sketch of pulsating pressure without sidewalls (Left: top view; Right: front view).

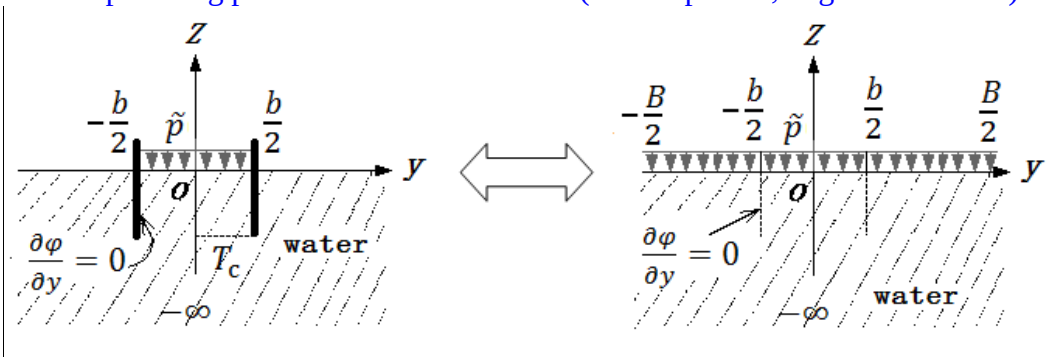

Fig. 5. Illustration of approximation to the problem induced by the pressure patch between sidewalls (Left) using an extended pressure patch without sidewalls but having infinite breadth.

The governing equations for this BVP are described by Eq.(A-5) in Appendix I, which are similar to these for wavemaker-with-lip problem in Ogilvie [18]. The major difference between Eq.(A-5) and the counterparts in Ogilvie [18] is that Eq.(A-5) describes a 3D problem about the pulsating pressure with a forward speed while those equations in Ogilvie [18] were for a two-dimensional (2D) problem about the pulsating pressure without a forward speed.

Refs. [14-17] solved a problem considering the traveling pulsating pressure but they all disregarded the sidewall condition, i.e., without imposing the third equation of Eq.(A-5) or assuming that the depth of the sidewall to be zero (see Fig. 4). Excluding the effect of sidewalls, the generated waves by the pulsating pressure can spread outward without being subjected to blocking or disturbing of the demihulls. In this paper, another approach is proposed based on the following assumptions. Firstly, the waves on the interface are propagating along the longitudinal direction rather than other

ones. Under this assumption, the demihulls can be simplified to thin plates, which are sufficient to reproduce the sidewall blocking effect. Of course, the plump demihulls are not thin and might have other effects on the waves on the interface, but in this paper those effects are considered to be of minor importance as compared to the blocking effect. Secondly, the 3D waves on the interface due to the pulsating air pressure can be further simplified to the 2D ones (it is rational because the length to beam ratio of the PACSCAT air cushion is more than 10:1), i.e. there is no transverse velocity component for the waves on the interface. Thus the problem can be simplified to a 2D pressure patch with infinite beam (denoted by B) moving along the longitudinal direction and producing 3D waves (long-crested waves).

For this purpose, the breadth of the pressure patch is extended from b (real beam of the air cushion) to B (right of Fig. 5). On this basis Eq.(A-5) is simplified as

$$\begin{cases} \nabla^2\varphi = 0, & z < 0, t > 0 \\ \left(\frac{\partial}{\partial t} - U\frac{\partial}{\partial x}\right)^2\varphi + \mathrm{g}\frac{\partial\varphi}{\partial z} = \begin{cases} -\left(\frac{\partial}{\partial t} - U\frac{\partial}{\partial x}\right)\tilde{p}(x,t)/\rho_{\mathrm{w}}, \\ 0, \end{cases} & \begin{matrix} |x| \le \frac{l}{2}, |y| \le \frac{B}{2} (z = 0, t > 0) \\ \text{otherwise} (z = 0, t > 0) \end{matrix} \\ \varphi = \partial\varphi/\partial t = 0, & z = 0, t \le 0 \\ \varphi, \partial\varphi/\partial r \to 0, & r \to \infty \end{cases} \tag{10}$$

Theoretically, if $B \to \infty$, $\partial\varphi/\partial y = 0$ at $|x| \le l/2$, $|y| \to (b-)/2$ and $(b+)/2$. In other words, the velocity potential does not change with y, and so the normal velocity to the sidewalls is zero near them, that is the condition on the sidewall is implicitly satisfied and the problem defined by Eq. (10) is similar to that defined by Eq. (A-5). However, there is a difference between the problem defined by Eq. (10) and that by Eq. (A-5). In Eq. (10) the normal velocity on the sidewalls is zero in the region $z < 0$, implying that the thin plates corresponding to the demihulls are modelled as infinitely deep, while in Eq. (A-5), $\partial\varphi/\partial y = 0$ is required for $-T_{\mathrm{c}} < z < 0$. Nevertheless, this difference will not cause the significant difference in the wave elevation under the air cushion. That is because the velocity potential φ reduces exponentially in terms of water depth ($\varphi \propto \mathrm{e}^{kz}$), so the error due to the difference should become smaller with the increase of the depth of the two thin plates or reduction of wave lengths. In this sense, the BVP in Eq. (10) is a fair approximation to the problem in Eq.(A-5). In computational practice, B must be finite but as long as it is large enough, the wave elevation under the air cushion should not considerably depend on the specific value of B. In addition, if B is taken as b, Eq. (10) becomes Eq. (A-5) without its third equation (in the other word, corresponding to the zero depth of sidewalls and the same as the models in Xie et al. [17]) while $B \to \infty$ corresponds to the case for an infinitely deep vertical walls. This may imply that the case with the sidewalls at a finite depth should correlate with a finite value of B, though it is unknown. The proper value of B will be demonstrated by numerical tests represented in Section 4. One should notice, when $B > b$, the waves on the outside

free surface are not real and only the ones on the interface are valid.

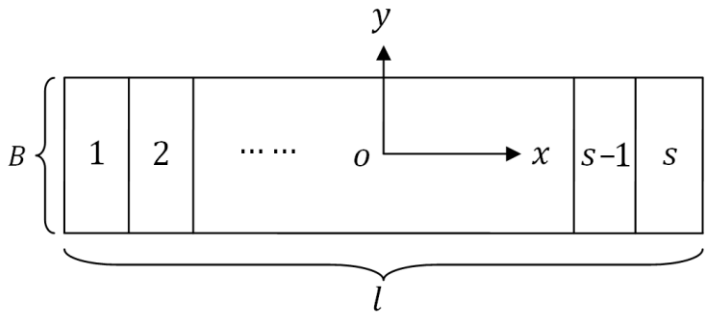

Fig. 6. Discretization of pressure patch with the width of *B*.

To solve the unsteady boundary value problem in Eq. (10), the spatially varying pulsating pressure patch $\tilde{p}(\xi,t)$ (Eq. (1)) with x replaced by ξ is decomposed into

$$\tilde{p}(\xi,t)=\sum_{j=0}^{s}\tilde{p}_j(\xi,t) \tag{11}$$

with

$$\tilde{p}_j(\xi,t)=\begin{cases}p_0\alpha e^{i\omega t}, & |\xi|\le l/2, & j=0\\ -\rho_0\beta e^{i\omega t}\sin\frac{\pi\left(j-\frac{s+1}{2}\right)}{s}, & \frac{l(2j-s-2)}{2s}\le\xi<\frac{l(2j-s)}{2s}, & j=1,2,\dots,s\\ 0, & \text{other}, & j=0,1,2,\dots,s\end{cases} \tag{12}$$

where $\tilde{p}_j(\xi,t),\ j=1,2,\dots,s$ is the discretization of the pressure patch $\tilde{p}(\xi,t)$ as illustrated in Fig. 6.

Assuming that $\zeta_j,\ j=0,1,2,\dots,s$ is the free surface elevation due to the pressure patch $\tilde{p}_j(\xi,t)$, and that $\zeta_r\left(x,y,t\middle|l_p,B;U;\tilde{p}_r(t)\right)$ $(B>b)$, where l_p denotes a length of discretized pressure patch and may or may not be equals to the length of the air cushion (l), is the free surface elevation at (x,y) due to the pressure patch $\tilde{p}_r(t)=e^{i\omega t}$ distributed on $l_p\times B$ and advancing with the forward speed U (Fig. 5), one, following Refs. [14,16], can obtain the following relationships between ζ_j and ζ_r:

$$\zeta_j=\begin{cases}p_0\alpha\cdot\zeta_r\left(x,y,t\middle|l,B;U;\tilde{p}_r(t)\right), & j=0\\ -\rho_0\beta\sin\frac{\pi\left(j-\frac{s+1}{2}\right)}{s}\cdot\zeta_r\left(x-\frac{l(2j-s-1)}{2s},y,t\middle|\frac{l}{s},\frac{B}{s};U;\tilde{p}_r(t)\right), & j=1,2,\dots,s\end{cases} \tag{13}$$

Consequently, the amplitude of the free surface elevation $\zeta_p(x,y)$ due to the whole pressure patch can be obtained by the linear superposition of ζ_j, i.e.

$$\zeta_p(x,y)=\sum_{j=0}^{s}\zeta_j=p_0\alpha\cdot\zeta_{p1}(x,y)+\rho_0\beta\cdot\zeta_{p2}(x,y) \tag{14}$$

with

$$\zeta_{pj}(x,y)=\begin{cases}\zeta_r\left(x,y,t\middle|l,B;U;\tilde{p}_r(t)\right), & j=1\\ \sum_{j=1}^{s}\sin\frac{\pi\left(\frac{s+1}{2}-j\right)}{s}\cdot\zeta_r\left(x-\frac{l(2j-s-1)}{2s},y,t\middle|\frac{l}{s},\frac{B}{s};U;\tilde{p}_r(t)\right), & j=2\end{cases}$$

Then the terms $\bar{\bar{\zeta}}_{\mathrm{p}}, \hat{\bar{\zeta}}_{\mathrm{p}}, \bar{\zeta}_{\mathrm{p}}(x)$ in Eq.(14) are approximated by

$$\begin{cases} \bar{\bar{\zeta}}_{\mathrm{p}} = p_0\alpha \cdot \bar{\bar{\zeta}}_{\mathrm{p1}} + \rho_0\beta \cdot \bar{\bar{\zeta}}_{\mathrm{p2}} \\ \hat{\bar{\zeta}}_{\mathrm{p}} = p_0\alpha \cdot \hat{\bar{\zeta}}_{\mathrm{p1}} + \rho_0\beta \cdot \hat{\bar{\zeta}}_{\mathrm{p2}} \\ \bar{\zeta}_{\mathrm{p}}(x) = p_0\alpha \cdot \bar{\zeta}_{\mathrm{p1}}(x) + \rho_0\beta \cdot \bar{\zeta}_{\mathrm{p2}}(x) \end{cases} \tag{15}$$

with

$$\begin{cases} \bar{\bar{\zeta}}_{\mathrm{p}j} = \frac{1}{A}\int_{-\frac{l}{2}}^{\frac{l}{2}}\int_{-\frac{b}{2}}^{\frac{b}{2}} \zeta_{\mathrm{p}j}(x,y)\mathrm{d}y\,\mathrm{d}x, \\ \hat{\bar{\zeta}}_{\mathrm{p}j} = \frac{1}{A}\int_{-\frac{l}{2}}^{\frac{l}{2}}\int_{-\frac{b}{2}}^{\frac{b}{2}} \zeta_{\mathrm{p}j}(x,y)\sin\frac{\pi x}{l}\mathrm{d}y\,\mathrm{d}x, \qquad j = 1,2 \\ \bar{\zeta}_{\mathrm{p}j}(x) = \frac{1}{b}\int_{-\frac{b}{2}}^{\frac{b}{2}} \zeta_{\mathrm{p}j}(x,y)\mathrm{d}y, \end{cases} \tag{16}$$

The detailed expressions for ζ_{r} can be found in Refs. [14,16].

3.2 Hydrodynamic BVP for the demihulls

The hydrodynamics of demihulls are associated with two aspects: (a) the hydrodynamic forces such as F_3^{R}, F_3^{W}, F_5^{R} and F_5^{W} involved in Eqs.(1)-(2), and (b) the waves induced by the demihulls under the air cushion. The hydrodynamic forces can be obtained by solving Eq.(A-4) using the high efficient 2.5D method as detailed in Duan et al. [20] and summarized in Guo et al. [3]. Here we mainly focus attention on the second aspect.

As indicated above, we only consider the waves excited by heave and pitch of the demihulls. In line with the linearized assumption these waves can be written as

$$\zeta_{\mathrm{h}}(x,y) = \zeta_{\mathrm{h3}}(x,y)\cdot\eta_3 + \zeta_{\mathrm{h5}}(x,y)\cdot\eta_5 + \zeta_{\mathrm{h7}}(x,y)\cdot\zeta_{\mathrm{a}} \tag{17}$$

where $\zeta_{\mathrm{h3}}(x,y)$, $\zeta_{\mathrm{h5}}(x,y)$ are the complex amplitude of radiation waves due to the heave and pitch of demihulls with a unit amplitude, respectively; $\zeta_{\mathrm{h7}}(x,y)$ is the complex amplitude of diffraction waves due to the disturbance of demihulls to incoming waves. Let $\psi_j(x,y,z)$, $(j = 3,5,7)$ be the velocity potentials for these waves satisfying Eq.(A-4) in Appendix I. These potential can be solved by using the 2.5D (2D+t) theory described by Refs. [20,21]. Once the potentials $\psi_j(x,y,z)$, $j = 3,5,7$ are found, the waves disturbed by the demihulls can be evaluated by

$$\zeta_{\mathrm{h}}(x,y) = -\left(\mathrm{i}\omega - U\frac{\partial}{\partial x}\right)\frac{\psi_3(x,y,0)}{\mathrm{g}}\cdot\eta_3^{\mathrm{s}} - \left(\mathrm{i}\omega - U\frac{\partial}{\partial x}\right)\frac{\psi_5(x,y,0)}{\mathrm{g}}\cdot\eta_5^{\mathrm{s}} - \left(\mathrm{i}\omega - U\frac{\partial}{\partial x}\right)\frac{\psi_7(x,y,0)}{\mathrm{g}}\cdot\zeta_{\mathrm{a}} \tag{18}$$

where η_j^{s} is the amplitude of the heave or pitch motion η_j, i.e. $\eta_j = \eta_j^{\mathrm{s}}\mathrm{e}^{\mathrm{i}\omega t}$, $j = 3,5$.

Then the terms $\bar{\bar{\zeta}}_{\mathrm{h}}$, $\hat{\bar{\zeta}}_{\mathrm{h}}$ and $\bar{\zeta}_{\mathrm{h}}(x)$ in Eq. (14) can be expressed as

$$\begin{cases} \bar{\bar{\zeta}}_{\mathrm{h}} = \eta_3^{\mathrm{s}} \cdot \bar{\bar{\zeta}}_{\mathrm{h}3} + \eta_5^{\mathrm{s}} \cdot \bar{\bar{\zeta}}_{\mathrm{h}5} + \zeta_{\mathrm{a}} \cdot \bar{\bar{\zeta}}_{\mathrm{h}7} \\ \hat{\bar{\zeta}}_{\mathrm{h}} = \eta_3^{\mathrm{s}} \cdot \hat{\bar{\zeta}}_{\mathrm{h}3} + \eta_5^{\mathrm{s}} \cdot \hat{\bar{\zeta}}_{\mathrm{h}5} + \zeta_{\mathrm{a}} \cdot \hat{\bar{\zeta}}_{\mathrm{h}7} \\ \bar{\zeta}_{\mathrm{h}}(x) = \eta_3^{\mathrm{s}} \cdot \bar{\zeta}_{\mathrm{h}3}(x) + \eta_5^{\mathrm{s}} \cdot \bar{\zeta}_{\mathrm{h}5}(x) + \zeta_{\mathrm{a}} \cdot \bar{\zeta}_{\mathrm{h}7}(x) \end{cases} \tag{19}$$

with

$$\begin{cases} \bar{\bar{\zeta}}_{\mathrm{h}j} = -\frac{1}{A}\int_{-\frac{l}{2}}^{\frac{l}{2}}\int_{-\frac{b}{2}}^{\frac{b}{2}}\left(\mathrm{i}\omega - U\frac{\partial}{\partial x}\right)\frac{\psi_j(x,y,0)}{\mathrm{g}}\mathrm{d}y\,\mathrm{d}x, \\ \hat{\bar{\zeta}}_{\mathrm{h}j} = -\frac{1}{A}\int_{-\frac{l}{2}}^{\frac{l}{2}}\int_{-\frac{b}{2}}^{\frac{b}{2}}\left(\mathrm{i}\omega - U\frac{\partial}{\partial x}\right)\frac{\psi_j(x,y,0)}{\mathrm{g}}\cdot\sin\frac{\pi x}{l}\mathrm{d}y\,\mathrm{d}x, \qquad j = 3,5,7 \\ \bar{\zeta}_{\mathrm{h}j}(x) = -\frac{1}{b}\int_{-\frac{b}{2}}^{\frac{b}{2}}\left(\mathrm{i}\omega - U\frac{\partial}{\partial x}\right)\frac{\psi_j(x,y,0)}{\mathrm{g}}\mathrm{d}y, \end{cases} \tag{20}$$

3.3 Coupled dynamic equations for the PACSCAT

With solutions for the hydrodynamics of demihulls and the pulsating pressure in the air cushion one can give the dynamic motion equations for the PACSCAT coupled with the pulsating pressure in the air cushion. Then using the Newton's second law, the pulsating pressure terms can be eliminated to give

$$\begin{cases} \left(\mathrm{i}\omega\left(\frac{h}{\gamma(p_0+p_{\mathrm{a}})} - \bar{\bar{\zeta}}_{\mathrm{p}1}\right) + \frac{\frac{Q_0}{2} - p_0\left(\left(\frac{\partial Q_{\mathrm{in}}}{\partial p}\right)_0 + \frac{Q_0}{h_1}\bar{\zeta}_{\mathrm{p}1}\left(-\frac{l}{2}\right)\right)}{p_0 A}\right)\left(M\ddot{\eta}_3 - F_3^{\mathrm{R}} - F_3^{\mathrm{W}}\right) + A\left(1 - \bar{\bar{\zeta}}_{\mathrm{h}3}\right)\dot{\eta}_3 \\ + \left(\frac{\left(\frac{l}{2} - \bar{\zeta}_{\mathrm{h}5}\left(-\frac{l}{2}\right)\right)Q_0}{h_1} - \mathrm{i}\omega A\bar{\bar{\zeta}}_{\mathrm{h}5}\right)\eta_5 + \frac{\pi^2}{2l}\left(\frac{Q_0}{A}\left(\frac{1}{2p_0} - \frac{\bar{\zeta}_{\mathrm{p}2}\left(-\frac{l}{2}\right)}{h_1}\right) - \mathrm{i}\omega\bar{\bar{\zeta}}_{\mathrm{p}2}\right)\left(I_{55}\ddot{\eta}_5 - F_5^{\mathrm{R}} - F_5^{\mathrm{W}}\right) \\ + \frac{\left(1 - \bar{\zeta}_{\mathrm{h}3}\left(-\frac{l}{2}\right)\right)Q_0}{h_1}\eta_3 = \zeta_{\mathrm{a}}\left(\frac{2\mathrm{i}\omega b\sin\frac{kl}{2}}{k} + \frac{\left(\mathrm{e}^{-\mathrm{i}\frac{kl}{2}} + \bar{\zeta}_{\mathrm{h}7}\left(-\frac{l}{2}\right)\right)Q_0}{h_1} + \mathrm{i}\omega A\bar{\bar{\zeta}}_{\mathrm{h}7}\right)\mathrm{e}^{\mathrm{i}\omega t} \qquad \text{(a)} \\ \left(\frac{\pi^2 h}{4\mathrm{i}\omega l}\left(\frac{\pi^2}{\rho_0 l^2} - \frac{\omega^2}{\gamma(p_0+p_{\mathrm{a}})}\right) + \frac{\pi^2\left(Q_0 - p_0\left(\left(\frac{\partial Q_{\mathrm{in}}}{\partial p}\right)_0 + \frac{2Q_0}{h_1}\bar{\zeta}_{\mathrm{p}2}\left(-\frac{l}{2}\right)\right)\right)}{4p_0 Al} + \frac{\mathrm{i}\omega\pi^2}{2l}\hat{\bar{\zeta}}_{\mathrm{p}2}\right)\left(I_{55}\ddot{\eta}_5 - F_5^{\mathrm{R}} - F_5^{\mathrm{W}}\right) \\ + \left(\frac{Q_0}{A}\left(\frac{1}{2p_0} - \frac{\bar{\zeta}_{\mathrm{p}1}\left(-\frac{l}{2}\right)}{h_1}\right) + \mathrm{i}\omega\hat{\bar{\zeta}}_{\mathrm{p}1}\right)\left(M\ddot{\eta}_3 - F_3^{R} - F_3^{W}\right) + \frac{\left(\frac{l}{2} - \bar{\zeta}_{\mathrm{h}5}\left(-\frac{l}{2}\right)\right)Q_0}{h_1}\eta_5 + A\left(\frac{2l}{\pi^2} + \hat{\bar{\zeta}}_{\mathrm{h}5}\right)\dot{\eta}_5 \\ + \left(\frac{\left(1 - \bar{\zeta}_{\mathrm{h}3}\left(-\frac{l}{2}\right)\right)Q_0}{h_1} + \mathrm{i}\omega A\hat{\bar{\zeta}}_{\mathrm{h}3}\right)\eta_3 = \zeta_{\mathrm{a}}\left(\frac{2\zeta_{\mathrm{a}}kAl\omega\cos\frac{kl}{2}}{\pi^2 - k^2 l^2} + \frac{\left(\mathrm{e}^{-\mathrm{i}\frac{kl}{2}} + \bar{\zeta}_{\mathrm{h}7}\left(-\frac{l}{2}\right)\right)Q_0}{h_1} - \mathrm{i}\omega A\hat{\bar{\zeta}}_{\mathrm{h}7}\right)\mathrm{e}^{\mathrm{i}\omega t} \qquad \text{(b)} \end{cases} \tag{21}$$

Eq.(21) is the final form of dynamic equations for the PACSCAT, which is linear in terms of the motion parameters of the PACSCAT and can be solved in the frequency domain. Once the motions of the PACSCAT are solved, the air cushion pressure can obtained using Eq. (1).

4. Numerical results and discussions

In this section, the numerical method described above will be validated, and the influence of the air cushion-water interaction on the PACSCAT seakeeping properties is investigated. As seen in Fig. 1, when the PACSCAT runs in waves, the sinkage and trim of the hull are different from those at the static floating condition. Therefore, the average sinkage and trim of the PACSCAT that were obtained from the experimental data [3] (see Table 1) are taken into account in the numerical practice. As discussed in the Section 3, the water level difference between the free surface and interface is not considered in this paper and the interface is set on the level of the free surface.

4.1 Free surface elevations due to pulsating air pressure

The first case is the one similar to that presented by Refs. [14,17], which has a square pressure patch ($p = |p|\mathrm{e}^{\mathrm{i}\omega t}$) traveling with a speed corresponding to the Froude number $F_{\mathrm{rL}} = U/\sqrt{2gl} = 0.5$ and the reduced frequency $\tau = U\omega/\mathrm{g} = 0.275$. As indicated before, the depth of the sidewalls was assumed to be zero in the cited paper, which corresponds to $B = b$ in our formulation. Real (Re) and imaginary (Im) parts of wave profiles ζ_{r} at $y/b = 1/2$ are compared in Fig. 7 with those of Refs. [14,17] for the same case. It can be seen that the agreement is quite good.

To investigate the influence of the sidewalls, the next case studied is similar to the above but with the parameters to be the same as these for the PACSCAT given in Table 1, that is, $\tau = 1.36$ ($U = 3.6\mathrm{m/s},\ \lambda = 14\mathrm{m}, \omega = 3.71\mathrm{rad/s}$) to 6.00 ($U = 5.0\mathrm{m/s},\ \lambda = 4\mathrm{m}, \omega = 11.8\mathrm{rad/s}$), and the pressure patch $p = |p|\mathrm{e}^{\mathrm{i}\omega t}$ defined over $l \times b = 2.5\mathrm{m} \times 0.24\mathrm{m}$. The maximum amplitudes of interface elevation at $y = 0$ due to the pulsating pressure $p = |p|\mathrm{e}^{\mathrm{i}\omega t}$ are shown in Fig. 8a. In the figure the label 'w/o' indicates the size of the pressure patch in the calculation is the same as the air cushion, i.e. $B = b$, while the label 'w' means that the size of pressure patch in the calculation is $2.5\mathrm{m} \times 240\mathrm{m}$, i.e. $B = 240\mathrm{m}$. From Fig. 8, one can find that if the sidewall effect is not considered, the free surface elevation under the air cushion would be very different from that with the sidewall effect.

The expression of pulsating air cushion pressure in Eq.(1) and Eq.(14) is the linear combination of two terms $\mathrm{e}^{\mathrm{i}\omega t}$ and $\mathrm{e}^{\mathrm{i}\omega t}\sin(\pi x/l)$. The effect of the former has been demonstrated above. The influence of the latter on the air-water interaction is shown in Fig. 8b, where the maximum amplitude of the interface elevation at $y = 0$ due to the pulsating pressure $p = |p|\mathrm{e}^{\mathrm{i}\omega t}\sin(\pi x/l)$ (other parameters are the same as in Fig. 8a) is plotted. One can find from Fig. 9 that there is also a significant difference between the results with and without considering the sidewall effects. More tested results about the different values of B will be given later.

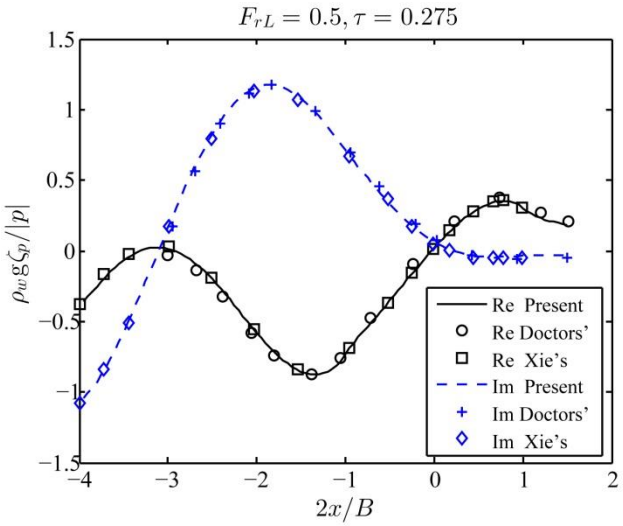

Fig. 7. Non-dimensional free-surface elevation at $y/b = 1/2$ due to the pulsating rectangular pressure patch $p = |p|e^{i\omega t}$ defined over $l/b = 1$ and $b/B = 1$.

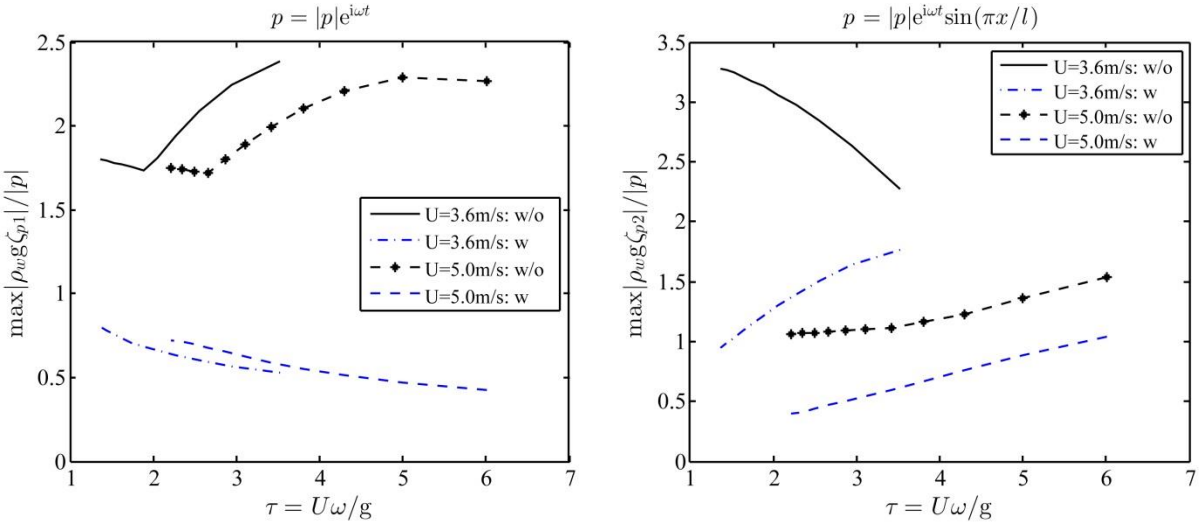

(a) (b)

Fig. 8. Maximal amplitude of non-dimensional wave elevation at $y = 0$ due to the pulsating rectangular pressure patch: (a) $p = |p|e^{i\omega t}$; (b) $p = |p|e^{i\omega t}\sin\frac{\pi x}{l}$. The legends 'w/o' means $B = 0.24$m while 'w' means $B = 240$m (B is the breadth of pressure patch involved in Eq.(13)).

4.2 Free surface elevations due to the forced motions of demihulls

The relative importance of the interface elevations due to the forced harmonic heave and pitch of PACSCAT demihulls and due to the diffraction of incident waves are investigated using the 2.5D method. Fig. 9a and 9b depict the wave profiles at $y = 0$ corresponding to the different reduced frequencies, respectively. One can observe that the magnitudes of the components are at the same order as incident waves and so there is no obvious reason for considering only one and ignoring others.

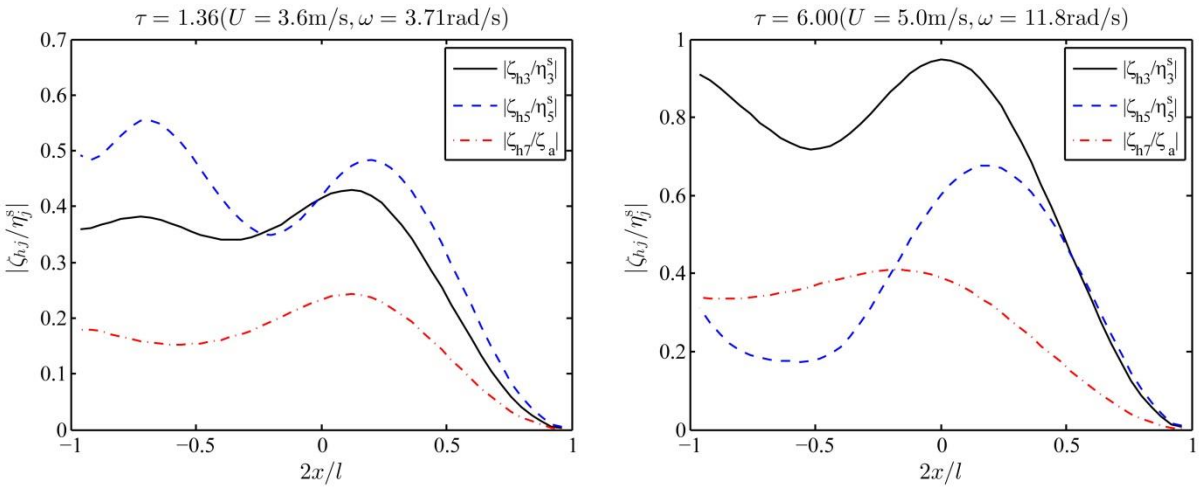

(a) (b)

Fig. 9. Amplitude of interface elevation at $y = 0$ due to the forced harmonic heave and pitch of PACSCAT demihulls and the diffraction of incident wave with unit amplitude.

4.3 Influence of the air cushion-water interaction on the seakeeping performance

As indicated in Fig. 8, the wave profiles between the demihulls can be very different for different values of B, i.e., with or without considering demihull's effects when evaluating the waves due to the air cushion pressure. It may be more interesting to look at how the value of B affects the seakeeping performance. For this purpose, the developed method is applied to simulating the cases corresponding to model tests on the PACSCAT with the parameters given in Table 1, presented in Guo et al. [3]. Some results are plotted in Fig. 10, together with the results from model tests [3] denoted by "EFD" (Experimental Fluid Dynamics).

Fig. 10a shows the results of heave RAOs (Response Amplitude Operators) for Froude number to be 1.0, predicted by setting different values of B from 0.24m to 5m. The case for $B = 0.24\text{m} = b$ corresponds to the case 'without sidewall effect' in Fig. 8, which actually corresponds to the model used, e.g., by Ref. [17], for evaluating the waves due to the air cushion pressure. As can be seen, the heave RAOs do not vary significantly when $B \geq 2.4\text{m}$. Fig. 10b depicts the pressure RAOs in the air cushion for the same cases in Fig. 10a. As can be seen, the pressure always increase with the increase of B, though the rate is reduced when $B \geq 2.4\text{m}$. Based on the facts in the two figures, we may consider $B = 2.4\text{m}$ to be appropriate for this PACSCAT as it leads to acceptable results compared with the experimental data. Nevertheless, the value of B can be different for different vehicles and can only be selected by numerical tests as done here. Fortunately, the numerical method is very efficient and takes only a few minutes of normal PCs to obtain the data for all the curves in the figures.

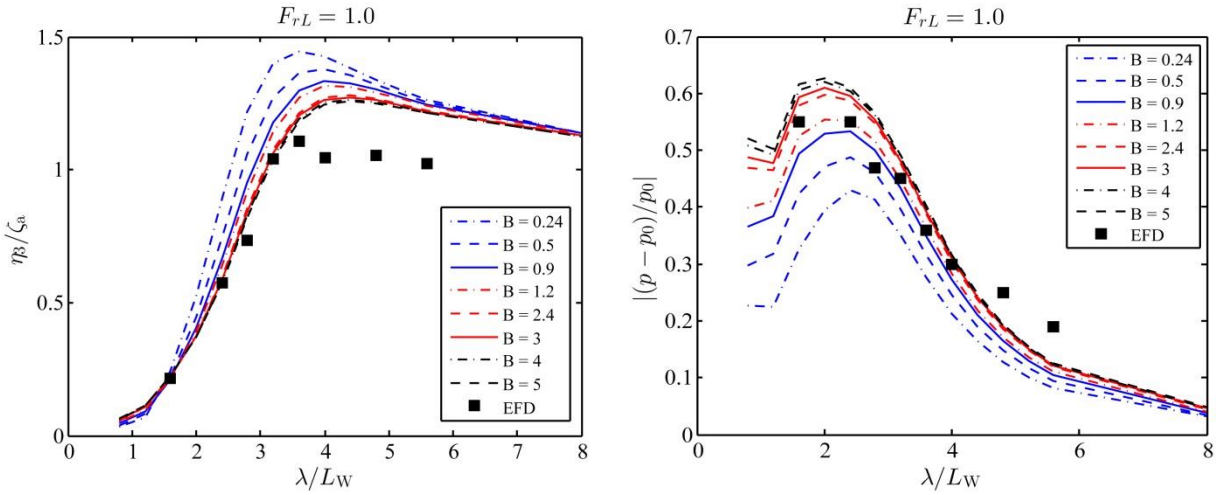

(a) Heave RAO (b) Air cushion pulsating pressure RAO

Fig. 10. Heave and air cushion pulsating pressure RAOs corresponding to different values of *B* (the breadth of pressure patch involved in Eq. (13)) and compared with EFD .

Using different approximations to evaluate the waves under the air cushion, four models may be formulated: (1) the model that only consider the incident wave but does not consider the air cushion-water interaction (labeled by "ζ_I"), which was used by Refs. [3,9-13]; (2) the model considers interface elevation due to the pulsating air pressure but does not take the sidewall effect into account (labeled by "$\zeta_I + \zeta_P$", corresponding to *B*=*b* as pointed above), which was utilized by Refs. [14-17]; (3) the model considers interface elevation due to pulsating air pressure with the sidewall effect (labeled by "$\zeta_I + [\zeta_P]$" corresponding to $B = 2.4$m for the PACSCAT in this paper (but the value of *B* can be different for others); (4) the model considers interface elevations due to the pulsating air pressure (the same as in Model (3)) and also due to the disturbance of the demihulls (labeled by "$\zeta_I + [\zeta_P] + \zeta_H$"). The last two models can only be formed from the method proposed in this work. The RAOs of heave, pitch and air cushion pulsating pressure for the Froude numbers of 0.73 and 1.0 using aforementioned 4 models are depicted in Figs. 11~ 13, respectively.

Fig. 11 shows that the model "$\zeta_I + \zeta_P$" overestimate the heave RAO particularly in the range of $\lambda/L_w = 2$ to 4. In contrast, the numerical results of the heave RAO from the models "ζ_I", "$\zeta_I + [\zeta_P]$" and "$\zeta_I + [\zeta_P] + \zeta_H$" have better agreement with the EFD data in general. More specifically, the heave RAO from the model "$\zeta_I + [\zeta_P] + \zeta_H$" agrees better with EFD data than those from the models "ζ_I" and "$\zeta_I + [\zeta_P]$" in short waves. However, the model "$\zeta_I + [\zeta_P] + \zeta_H$" does not outperform the models "ζ_I" and "$\zeta_I + [\zeta_P]$" in long waves or low encountered frequencies, which might be due to the fact that the 2.5D theory is based on the high frequency assumption ($\omega = O(1/\sqrt{\varepsilon})$, where ε has the same order as the ratio of the demihull's beam to length). The numerical results of pitch RAO in Fig. 12 illustrate that different models lead to roughly similar pitch motion.

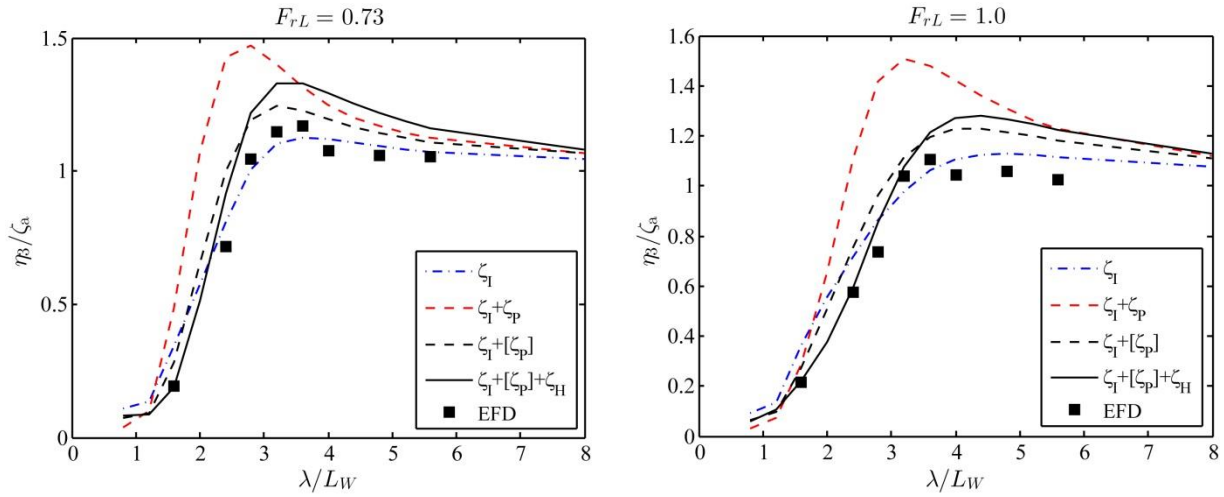

Fig. 11. Heave RAOs from 4 different models and compared with EFD

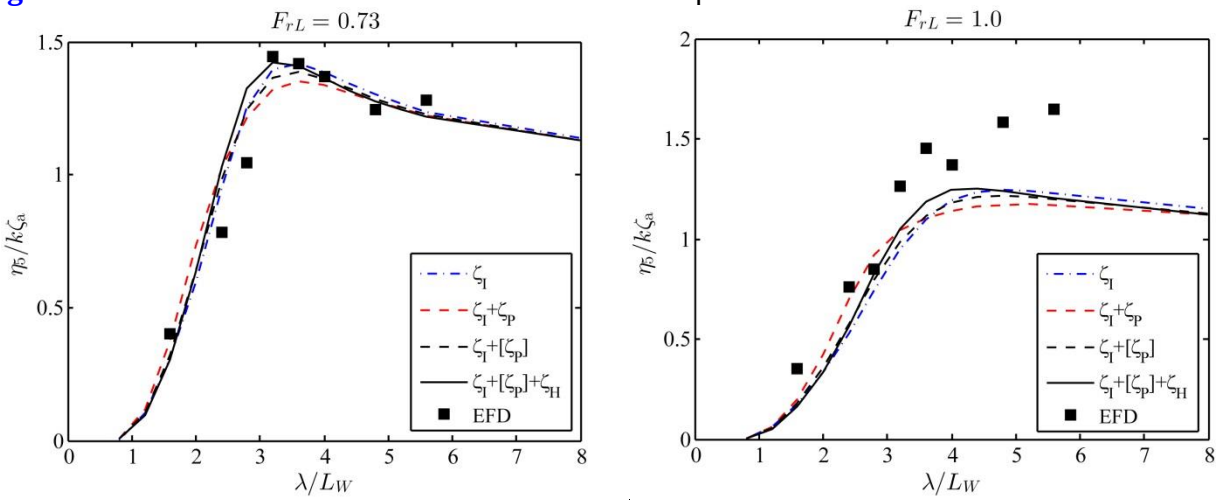

Fig. 12. Pitch RAOs from 4 different models and compared with EFD

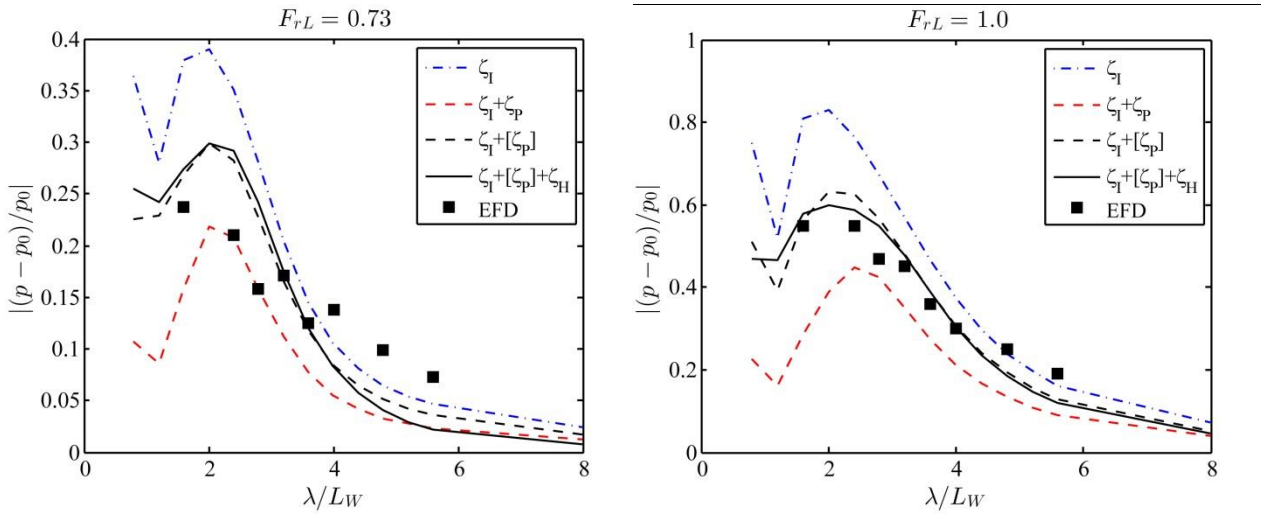

Fig. 13. Air cushion pulsating pressure RAOs from 4 different models and compared with EFD

Fig. 13 suggests that the models "$\zeta_I + [\zeta_P]$" or "$\zeta_I + [\zeta_P] + \zeta_H$" can always give better prediction to the pressure RAO than the model "ζ_I". Meanwhile, the consideration of "ζ_H" can slightly improve the numerical result of the pressure RAO. It is interesting to see that the results for the

pressure RAO predicted by the model "$\zeta_I + \zeta_P$" ($B = b$) are also not far from the EFD data, though it underestimates the pressure RAO, in contrast to its over-prediction of heave RAOs.

One may note that there is still a quite notable discrepancy in the pitch motion between the EFD data and the results from all the models when the Froude number and wave length are both large ($F_{rL} = 1.0,\ \lambda/L_w > 4$). This might be due to ignoring the effects of the stern lobe dynamics. The study of stern lobe dynamics will be carried out in the future.

5. Conclusions

This paper presents an improved method for evaluating the hydrodynamics of the air cushion of a high-speed PACSCAT. This is a simplified but an efficient method. It is different from existing methods in the following three aspects. (1) The current method takes the waves induced by the pulsating air pressure into account and couples it with the hydrodynamics of demihulls and air dynamics of the air cushion in contrast with the methods for ACV or SES that are based on the Froude-Krylov hypothesis [3,9-13]. (2) The method proposed here counts for the effects of demihulls on the waves induced by the air pressure in the air cushion while the methods proposed by Refs. [15-17] partially considered the air cushion-water interaction. (3) Compared with the computational methods that might be able to precisely simulate the air cushion-water-demihull interaction [4-7], the current method is more computationally efficient.

The improved method can give numerical results that are closer to EFD data, in particular for pressure RAOs, than the method developed in Guo et al. [3], where only the incident waves are considered when evaluating the pressure in the air cushion. Nevertheless, the difference between numerical and experimental pressure RAOs are still quite notable. That is perhaps because of the assumption that the demihulls are replaced by the sidewalls when evaluating the wave elevation under the air cushion. In reality, the demihulls with the finite thickness and depth may have the different effect from the sidewalls that is infinitely deep and thin. In addition, the improvement on the pitch motion is not significant. That is perhaps due to the fact that the dynamics of the flexible seals is ignored in the current method.

Acknowledgements

This project is supported by the National Natural Science Foundation of China (Grant, no.51509053, no. 51739001 and no.51579056), the Ship Industry Foundation Funds under Grant 14J1.2.3 and the Fundamental Research Funds for the Central Universities under Grant HEUCFM160104. The third author wishes to thank the Chang Jiang Visiting Chair professorship of Chinese Ministry of Education, supported and hosted by the HEU.

References

[1] J.C. Harris, S.T. Grilli, Computation of the wavemaking resistance of a Harley surface effect ship, in: 17th International Offshore and Polar Engineering Conference (ISOPE 2007), July 1−6, Lisbon, Portugal (2007) 3732-3739.

[2] A.F. Molland, P.A. Wilson, J.C. Lewthwaite, D.J. Taunton, An investigation into the hydrodynamic characteristics of a high-speed partial air cushion supported catamaran (PACSCAT), in: 8th International Conference on Fast Sea Transportation (FAST 2005), June 27-30, Saint-Petersburg, Russia, 2005.

[3] Z.Q. Guo, Q.W. Ma, J.L. Yang, A seakeeping analysis method for a high-speed partial air cushion supported catamaran (PACSCAT), Ocean Eng. 110 (2015) 357-376.

[4] S.B. Connell, M.W. Milewski, B. Goldman, C.D. Kring, Single and multi-body surface effect ship simulation for T-Craft design evaluation, in: 11th International Conference on Fast SeaTransportation (FAST 2011), September 26-29, Honolulu, Hawaii, USA (2011) 130-137.

[5] S. Zhang, K. Weems, W.M. Lin, Solving nonlinear wave-body interaction problems with the pre-corrected fast Fourier transform (pFFT) method, in: 11th International Conference on Fast Sea Transportation (FAST 2011), September 26-29, Honolulu, Hawaii, USA (2011) 153-160.

[6] S. Bhushan, F. Stern, L.J. Doctors, T-Craft calm water resistance and motions, and seakeeping in regular waves, in: 11th International Conference on Fast Sea Transportation (FAST 2011), September 26-29, Honolulu, Hawaii, USA (2011) 74–81.

[7] S. Bhushan, M. Mousaviraad, F. Stern, Assessment of URANS surface effect ship models for calm water and head waves, Appl. Ocean Res. 67 (2017) 248-262.

[8] Z.Q. Guo, Q.W. Ma, H.D. Qin, A novel 2.5D method for solving the mixed boundary value problem of a surface effect ship, Appl. Ocean Res. 78 (2018) 25-32.

[9] O.M. Faltinsen, Hydrodynamics of high-speed marine vehicles, Cambridge University Press, 1st ed., New York, NY, USA (2005) 141– 163.

[10] R.M. Dhanak, SES seakeeping motion in transforming near-shore head seas, in: 11th International Conference on Fast Sea Transportation (FAST 2011), September 26-29, Honolulu, Hawaii, USA (2011) 74-81.

[11] A.J. Sørensen, O. Egeland, Design of ride control system for surface effect ships using dissipative control, Auromadca 31(2) (1995) 183-199.

[12] L. Yun, A. Bliault, Theory and design of the air cushion craft, First published in Great Britain in by Arnold, a member of the Hodder Headline Group, 338 Huston Road, London NW1 3BH, 2000.

[13] N. Liu, X.Q. Wang, H.L. Ren, L.B. Zhuge, Nonlinear theory research on motion response of the

air cushion vehicle in waves, J. Huazhong Univ. of Sci. & Tech. (Natural Science Edition) 42(4) (2014) 91-95 (in Chinese).

[14] L.J. Doctors, The hydrodynamic influence on the non-linear motion of an ACV over waves, in: 10th Symposium on Naval Hydrodynamics, June 24-28, Cambridge, Massachusetts (1974) 389-420.

[15] L.J. Doctors, The effect of air compressibility on the nonlinear motion of an air-cushion vehicle over waves, in: 11th ONR Symposium on Naval Hydrodynamics, 28 March - 2 April, UCL, London, UK (1976) 373–388.

[16] C.H. Kim, S. Tsakonas, An analysis of heave added mass and damping of a surface-effect ship, J. Ship Res. 25(1) (1981) 44-61.

[17] N. Xie, D. Vassalos, A. Jasionowski, P. Sayer, A seakeeping analysis method for an air-lifted vessel, Ocean Eng. 35 (2008) 1512-1520.

[18] T.F. Ogilvie, Pulsating pressure fields on a free surface, AD0698846, Department of Naval Architecture, The University of Michigan, Ann Arbor, Michigan, USA, 1969.

[19] Z.Q. Guo, Q.W. Ma, H.B. Sun, H.B. Hao, 2.5D method for pulsating pressure induced waves on the free surface, in: 27th International Ocean and Polar Engineering Conference (ISOPE 2017), June 25-30, San Francisco, California, USA (2017) 1029-1033.

[20] W.Y. Duan, D.A. Hudson, W.G. Price, Theoretical prediction of the motions of fast displacement vessels in long-crested head seas, in: 3rd International Conference for High Performance Marine Vehicles, Shanghai, The Royal Institution of Naval Architects, 2000.

[21] S. Ma, W.Y. Duan, J.Z. Song, An efficient numerical method for solving ‘2.5D’ ship seakeeping problem, Ocean Eng. 32(8-9) (2005) 937-960.

Appendix I Linear hydrodynamic boundary value problems for the PACSCAT

Assuming that the total velocity potential in the water flow field is

$$\Psi = \psi_0 + \Phi \tag{A-1}$$

where ψ_0 is the velocity potential of incident waves; Φ is the velocity potential of water disturbed by the PACSCAT, including its hulls and air cushion. Using the linear assumption, the hydrodynamic boundary value problem for the velocity potential can be written as

$$\begin{cases} \nabla^2\Phi = 0, & z < 0, t > 0 \\ \left(\frac{\partial}{\partial t} - U\frac{\partial}{\partial x}\right)^2 \Phi + \mathrm{g}\frac{\partial \Phi}{\partial z} = \begin{cases} -\frac{\left(\frac{\partial}{\partial t} - U\frac{\partial}{\partial x}\right)\tilde{p}(x,t)}{\rho_w}, \\ 0, \end{cases} & \begin{matrix} \text{on interface} \\ \text{on free surface} \end{matrix} \\ \frac{\partial \Phi}{\partial n} = \sum_{j=1}^{6}(\dot{\eta}_j n_j + U\eta_j m_j) - \frac{\partial \psi_0}{\partial n}, & \text{on demihulls} \\ \Phi = \frac{\partial \Phi}{\partial t} = 0, & z = 0, t \le 0 \\ \text{Far field boundary conditions} \end{cases} \tag{A-2}$$

where U is the speed of the PACSCAT; $z = 0$ is the mean water level; ρ_w is the water density; n_j are the generalized normal vectors for the wetted surface, $(n_1, n_2, n_3) = \vec{n}$, $(n_4, n_5, n_6) = \vec{r} \times \vec{n}$, where $\vec{n}$ is a unit normal vector outward from the mean wetted surface of the vessel, $\vec{r}$ is a position vector of a point on the mean wetted surface; m_j are the coupling coefficients of steady and disturbed potentials, which are given by $(m_1, m_2, m_3) = (0,0,0)$, $(m_4, m_5, m_6) = (0, n_3, -n_2)$ (Ma, 2005).

Due to the linear assumption, the velocity potential Φ may be decomposed into 2 components corresponding to different boundary conditions, i.e.

$$\Phi = \varphi + \psi\ . \tag{A-3}$$

where φ is the velocity potential due only to the pressure in the air cushion with the hull fixed and without incident waves; ψ is the velocity potential due to the hull and its motions as well as incident waves but the pressure in the air cushion is equal to atmospheric pressure, i.e. corresponding to the diffraction and radiation of hulls. The boundary value problem for ψ can be expressed as

$$\begin{cases} \nabla^2\psi = 0, & z < 0, t > 0 \\ \left(\frac{\partial}{\partial t} - U\frac{\partial}{\partial x}\right)^2 \psi + \mathrm{g}\frac{\partial \psi}{\partial z} = 0, & \text{on free surface} \\ \frac{\partial \psi}{\partial n} = \sum_{j=1}^{6}(\dot{\eta}_j n_j + U\eta_j m_j) - \frac{\partial \psi_0}{\partial n}, & \text{on demihulls} \\ \psi = \frac{\partial \psi}{\partial t} = 0, & z = 0, t \le 0 \\ \text{Far field boundary conditions} \end{cases} \tag{A-4}$$

The velocity potential φ caused by the pulsating pressure in the air cushion should satisfy the condition on the fixed hull surfaces in addition to the free surface condition. For the simplicity and

for the sake of deriving the analytical solution, the hulls will be approximated by vertical plates with zero thickness. Thus the unsteady boundary value problem for φ can be written as

$$\begin{cases} \nabla^2\varphi = 0, & z < 0, t > 0 \\ \left(\frac{\partial}{\partial t} - U\frac{\partial}{\partial x}\right)^2 \varphi + g\frac{\partial \varphi}{\partial z} = \begin{cases} -\frac{\left(\frac{\partial}{\partial t} - U\frac{\partial}{\partial x}\right)\tilde{p}(x,t)}{\rho_w}, \\ 0, \end{cases} & \begin{matrix} |x| \le \frac{l}{2}, |y| \le \frac{b}{2}, z = 0, t > 0 \\ |x| > \frac{l}{2} \text{ or } |y| > \frac{b}{2}, z = 0, t > 0 \end{matrix} \\ \frac{\partial \varphi}{\partial y} = 0, & |x| \le \frac{l}{2},\ |y| \to \frac{b-}{2} \text{and } \frac{b+}{2}, -T_c < z < 0 \\ \varphi = \frac{\partial \varphi}{\partial t} = 0, & z = 0, t \le 0 \\ \text{Far field boundary conditions} \end{cases} \tag{A-5}$$

where l and b is the length and beam of the air cushion, respectively; T_c is the average draught of sidewalls; the requirement of $|y| \to (b-)/2$ and $(b+)/2$ implies that $\partial\varphi/\partial y = 0$ satisfies on both sides of two plates.

In Eq.(A-2) and Eq.(A-5), the effect of the pulsating pressure induced velocity on the demihulls is neglected, since we have assumed that this effect is less important than the blocking effect of sidewalls. Moreover, in addition to the pulsating pressure $\tilde{p}(x,t)$ there is a time average pressure p_0 (called as the equilibrium pressure here) in the air cushion which may not be equal to the atmospheric pressure. Generally, the equilibrium pressure shall have a coupling with the unsteady flow even in the linearized framework, though which is considered to be nonsignificant in most studies. For the sake of simplicity, the coupling effects between steady and unsteady flows are also neglected in this paper.

As discussed above, the overall velocity potential of water can be written as $\Psi = \psi_0 + \varphi + \psi$. Correspondingly, the free surface elevation under the air cushion should be expressed by

$$\zeta = \zeta_I + \zeta_P + \zeta_H \tag{A-6}$$

where ζ_I, ζ_P, ζ_H are the free surface elevations due only to incident waves (ψ_0), pulsating pressure (φ) and the diffraction and radiation of the side-hulls (ψ), respectively.